

## TARGETED THERAPY FOR BREAST CANCER CELLS BY HERBAL DRUG FORMULATIONS OF IRON OXIDE NANOPARTICLES

SWATHY JS, PRASEETHA PK\*, SAKTHIVEL G

Department of Nanotechnology, Noorul Islam Centre for Higher Education, Kumaracoil, Thuckalay, Tamil Nadu - 629 180, India.  
Email: crkpkp@gmail.com

Received: 19 November 2015, Revised and Accepted: 27 November 2015

### ABSTRACT

**Objective:** Nanoparticle-based drug delivery is the currently focused area in case of various therapeutic and diagnostic techniques. Iron oxide nanoparticles are used as carriers in drug delivery due to their unique properties and negligible side effects.

**Methods:** We analyze the potential therapeutic properties of methanolic extracts of *Centella asiatica* loaded with polyvinylpyrrolidone (PVP) iron oxide nanoparticles against human breast cancer cell lines michigan cancer foundation - 7 type (MCF-7), and the results were compared with normal cell lines. Characterization of coated nanoparticles was done by ultraviolet - visible (UV-VIS) spectroscopy, Fourier transform infra-red spectroscopy (FTIR) and particle size analyzer. Loading of herbal drug extract to nanoparticles was confirmed using TEM, particle size analyzer, FTIR, and biochemical assays. Initially, dose-depended hydrogen peroxide free radical scavenging activity was recorded.

**Results:** Methanolic extracts of *C. asiatica* showed 55, 59, 71, and 80% inhibition, respectively. MTT assay (3-(4,5-dimethylthiazol-2-yl)-2,5-diphenyltetrazolium) was performed to estimate the drug loading efficiency for PVP-coated iron oxide nanoparticle at 1 hr and 24 hrs. At 10  $\mu$ l concentration, methanolic extracts of *C. asiatica* loaded PVP-coated iron oxide nanoparticles exhibited significant cell necrosis in breast cancer cell line MCF-7 as 60%. In the case of normal cell lines - fibroblast cell lines (L929), the cytotoxicity was reduced to 10.42, respectively.

**Conclusion:** This work was aimed to increase the efficiency, reduce side effects of chemotherapeutic drugs, and provide conveniences for the future therapeutics by coupling herbal drug with polymer-coated nanoparticles.

**Keywords:** Iron oxide nanoparticles, Chemotherapy, Herbal drug, Anticancer activity.

### INTRODUCTION

Breast cancer is a major public health problem in developed countries like the United States and rising issue in India [1,2]. It is the most common cancer in women and the leading cause of cancer death among women 25-60 years of age [3]. The international agency for research on cancer estimates 411,000 deaths occur among 1.15 million diagnosed cases [4]. The rising incidence and poor prognosis of breast cancer cases have prompted a search for additional preventive and the therapeutic modalities [5].

Nano-biotechnology is the most advancing field of nanoscience which involves nanoparticles for various biomedical applications and therapeutic treatment for cancers [6]. Due to unique biological effects nanoparticles show different molecular approach from traditional small molecules to complicated drugs [7]. European Science Foundation points out the need for larger investments in developing nanotechnological tools in diagnostics and therapeutics for various diseases [8]. The modern treatment for cancers shows several side effects and produce toxicity to both cancer and normal cells. Even chemotherapy is often limited by important side effects and is non-specific to cancer or tumor cells, leading to serious damage to healthy cells [9]. Nanoparticles coated with natural drugs are implemented as drug delivery for cancer treatment because of their intrinsic physical properties and their ability to target specific cancer tissues and prevent toxicity to healthy tissues [10,11].

Iron oxide nanoparticles are widely used drug delivery agents in cancer diagnosis [12]. Iron oxide nanoparticles have been applied as magnetic contrast agents for over 45 years. Now, it is successfully employed in the biomedical applications for blood pooling, tissue and as target cell specific agents for magnetic resonance imaging in cancer diagnostics [13]. Apart from several clinical applications of Iron oxide

nanoparticles, there are many reports about the toxicity produced by these nanoparticles when it interacts with biological systems. Iron oxide nanoparticles induced reactive oxygen species creating an oxidative stress on the cell which results in cytotoxicity. Oxidative stress caused by iron oxide nanoparticles will damage DNA and this damage to genetic content will lead to apoptosis. Nanoparticles coated with the polymer membrane show promising decrease or reduction in the toxicity and this method is widely followed in the field of drug delivery [14].

The scientific community is attracted toward medicinal plants as a source of drugs for various diseases and approximately 64% of the global population uses traditional medicine due to less cost and lower side effects compared to modern drugs [15]. *Centella asiatica* is widely used medicinal plants to treat various diseases [16]. *C. asiatica*, a plant of the family Umbelliferae, is commonly known as gotakola. It commonly grows in damp areas in tropical countries and is used traditionally as a multipurpose medicinal plant in the treatment of cancer, neuron diseases, wound healing, tuberculosis, lumps, etc [13]. The plant is widely used as a tonic in skin diseases and leprosy. In addition, the flavonoids of this plant have antiulcer, antitumor, and wound healing activity [17]. The present study aims to examine the potentials of *Rauwolfia serpentina* and *C. asiatica* as anticancer drugs loaded onto polymer-coated nanoparticles against human breast cancer cell lines michigan cancer foundation-7 (MCF-7).

Among the many polymers used as protective coating for drug delivery, PVP is most common due to its varied biological applications. PVP was reported as an effective plasma substitute due to its hydrophilic nature and non-toxicity. PVP-coated silver nanoparticles are already used in complicated cases of serious burns and purulent wounds due to its antiseptic properties [18]. Another report suggests that PVP-based

drug delivery enhanced gene expression in muscle tissue and also protect plasmid DNA from nuclease degradation [19]. PVP is known as a biologically friendly polymer. They are currently used in various biomedical applications such as the artificial pancreas, synthetic vitreous body, wound dressing, artificial skin, cardiovascular devices, and other biomedical applications [20]. Combining such properties of these polymer-coated nanoparticles along with the natural drug may lead to possible preparations of new effective drugs for cancer diagnostics. Nanoformulation of herbal extracts from *C. asiatica* is a novel study paving the way for new therapeutics based on herbal medicinal compounds.

## METHODS

### Plant extraction

The plant material *C. asiatica* were collected from the nearby Veli Hills and were identified and confirmed by Botanical experts. The fresh leaves were cleaned, shade dried, and reduced into a coarse powder in a Wiring blender. The plants powdered were subjected to soxhlet extraction (70±10°C temp.) with methanol as a solvent in 1: 4 (w/v) ratios for 18 hrs. The extracts were concentrated using a rotary vacuum evaporator (40°C; pressure 70±5 psi); thick, brown mass obtained was kept in vacuum desiccators for complete drying. The dried extracts were stored in an airtight container and kept in the refrigerator (8±2°C), and the same was used for *in vivo* and *in vitro* studies.

### Phytochemical screening

The preliminary phytochemical screening was carried out according to the procedure given by Harborne [21], which revealed the presence of lipids, carbohydrates, flavonoids, and alkaloids in both the plant extracts.

### *In vitro* antioxidant activity

The plant extracts were dissolved in 3, 4 ml of 0.1 mol phosphate buffer (pH-7.4) and mixed with 600 ml of 43 mmol solution of hydrogen peroxide. The absorbance value (at 230 nm) of the reaction mixture was recorded from 0 to 40 minutes and then at every 10 minutes. For each concentration, a separate blank sample was used for background subtraction. The percentage H<sub>2</sub>O<sub>2</sub> scavenging activity of the synthesized compounds and standard compound was calculated as:

$$\text{H}_2\text{O}_2 \text{ scavenging effect (\%)} = \left( \frac{[V_0 - V_1]}{V_0} \right) \times 100$$

Where,

V<sub>0</sub> = Absorbance of control

V<sub>1</sub> = Absorbance of the sample.

### Synthesis of iron oxide nanoparticles

The stock solution preparation includes: 3.85 g of ferric chloride was added to 50 ml of double distilled water to make a solution of 1 mol. 6 g of ferrous chloride was added to 50 ml of distilled water to make a solution of 2 mol. 2 g of NaOH was added to 50 ml of distilled water to make a solution. For preparing the iron oxide nanoparticles 8 ml of 1 mol ferric chloride and 2 ml of 2 mol ferrous chloride was mixed and stirred. While stirring NaOH solution was added drop by drop until the solution turned brown. After preparing iron oxide nanoparticles, 5 g of PVP was added and sonicated for 30 minutes. Then, the mixture was heated for 30 minutes at 600°C.

### Drug loading into PVP-coated and uncoated iron oxide nanoparticles

Drug loading can be done by two methods, i.e., incorporation and incubation. In these systems, the drug is embedded into the matrix or adsorbed onto the surface. The efficiency of loading is largely dependent on the method of preparation and physicochemical properties of the drug. The anticancer herbal drugs from *C. asiatica* were chosen as drugs. The drug loading was carried out by dispersing 5 mg of PVP-coated iron oxide nanoparticles in 5 ml aqueous plant extract solutions and 5 mg uncoated iron oxide 5 ml aqueous plant extract solutions consecutively. The mixture of PVP-coated iron oxide nanoparticles in herbal drug

(test solution) and PVP-uncoated iron oxide nanoparticles in herbal drug (control solution) can be shaken in a rotary shaker (200 rpm) at 37°C for 26 hrs. The drug loading can be determined as the difference between the initial drug concentration and the drug concentration in the supernatant. The drug loaded magnetic nanoparticles was then magnetically separated and dried.

$$\text{Loading Efficiency (\%)} = \frac{\text{UV absorbance of drug} - \text{UV absorbance of drug in supernatant}}{\text{UV absorbance of drug}}$$

## CHARACTERIZATION OF SYNTHESIZED, POLYMER COATED, AND UNCOATED NANOPARTICLES

### Fourier transform infra-red spectroscopy (FTIR) spectroscopy

The ATR-FTIR measurements were performed on a Bruker Eco Alpha-T FTIR spectrometer (Bruker, Karlsruhe, Germany) equipped with a mid-infrared source (SiC) and a thermal detector, such as deuterated, L-alanine doped triglycine sulfate premium performance pyroelectric detector. Spectra were collected at room temperature under atmospheric pressure, at an average of 64 scans with a resolution of 4/cm resolution in ATR mode from 400 to 5000/cm. In all experiments, background spectra were measured. FTIR spectroscopy measurements were carried out to recognize the chemical functional group in the sample. FTIR samples were prepared by drying sample with nanoparticles at 60°C. The dried samples were subjected to FTIR measurement.

### UV-visible spectroscopy

The UV/Vis spectra of surface plasmon resonances of iron oxide nanoparticles were analyzed using Systronics (India) double beam spectrophotometer (Model no. M2202). The range of measurement is taken from 200 to 1100 nm. Blanks were prepared with distilled and deionized (DI) water using a Milli-Q water purification system (Millipore Corp.).

### Particle size analyzer

The mean particle size of PVP-coated, uncoated iron, and drug-loaded nanoparticles was estimated using a particle size analyzer, DC 12000, CPS Instruments USA. Particle Analyzer is used to characterize the size distribution of particles in a given sample. Particle size analysis can be applied to solid materials, suspensions, emulsions, and even aerosols. There are many different methods employed to measure particle size.

### Transmission electron microscopy (TEM)

The size of PVP-coated, uncoated nanoparticles, and drug-loaded iron nanoparticles were visualized by TEM (Hitachi H-7650 Tokyo, Japan) operating at 80 kV. TEM is a microscopy technique whereby a beam of electrons is transmitted through an ultra-thin specimen, interacting with the specimen as it passes through. TEMs are capable of imaging at a significantly higher resolution than light microscopes, owing to the small de Broglie wavelength of electrons.

### *In vitro* cytotoxicity study

L929 Fibroblast cells and MCF-7 breast cancer cell lines were purchased from the National Centre for Cell Sciences (NCCS) Pune was maintained in Dulbecco's modified eagles media (HIMEDIA) supplemented with 10% fetal bovine serum (Invitrogen) and grown to confluency at 37°C in 5% CO<sub>2</sub> (NBS, EPPENDORF, GERMANY) in a humidified atmosphere in a CO<sub>2</sub> incubator. The cells were trypsinized (500 µl of 0.025% trypsin in PBS/0.5 Mm EDTA solution (Himedia) for 2 minutes and passaged to T-flasks in complete aseptic conditions. 1 µL, 5 µL, and 10 µL of extracts were added to grown cells and incubated for 24 hrs. The % difference in viability was determined by standard MTT assay after 24 hrs of incubation. The cell culture suspension was washed with ×1 PBS and then added 30 µl of the MTT solution to the culture (MTT -5mg/ml dissolved in PBS). It was then incubated at 37°C for 3 hrs. MTT was removed by washing with ×1 PBS, and 200 µl of dimethyl sulfoxide (DMSO) was added to the culture. Incubation was done at room temperature for 30 minutes until the cell got lysed and

color was obtained. The solution was transferred to centrifuge tubes and centrifuged at top speed for 2 minutes to precipitate cell debris. OD was read at 540 nm using DMSO as blank.

$$\% \text{ cell viability} = (\text{OD of test} / \text{OD of Control}) \times 100$$

## RESULTS

### Phytochemical screening

Terpenoids and indole alkaloid biochemical conformation tests were carried out with the extracts of *C. asiatica*. The presence of terpenoids was confirmed based on the reddish-brown coloration of the interface. Ehrlich test indicates the presence of indole alkaloids by the production of the red solution. The details of the study can be observed from Fig. 1.

### Antioxidant assay

Hydrogen peroxide scavenging property of *C. asiatica* 0.5, 1, 1.5, and 2 ml, respectively, was compared to the blank solution having phosphate buffer with  $\text{H}_2\text{O}_2$ . The antioxidant properties exhibited by the methanolic extract are represented in Fig. 2. At 230 nm absorbance, 80% hydrogen peroxide scavenging activity was absorbed for 2 ml concentration of *C. asiatica*.

### UV-visible spectroscopy

Fig. 3a represents the absorption of Iron oxide nanoparticles dispersed in water at the wavelength of 286 nm. The UV-vis spectra of PVP revealed an absorption peak at the wavelength 464 nm. Fig. 3b UV-vis absorption of PVP-coated iron oxide nanoparticles shows a strong absorption at 512 nm. The results correlated with previous observation. UV-vis spectra of the synthesized iron oxide nanoparticles were recorded. The absorption of iron oxide nanoparticles dispersed in water was at the wavelength of 286 nm. The spectrum obtained at nm represents the peak for PVP-coated Iron oxide nanoparticles. Fig. 3c denotes the UV-vis absorption of drug loaded PVP-coated iron nanoparticles shows a strong absorption at 572 nm.



Fig. 1: Salkowski confirmation test for tri-terpenoids and indole alkaloids

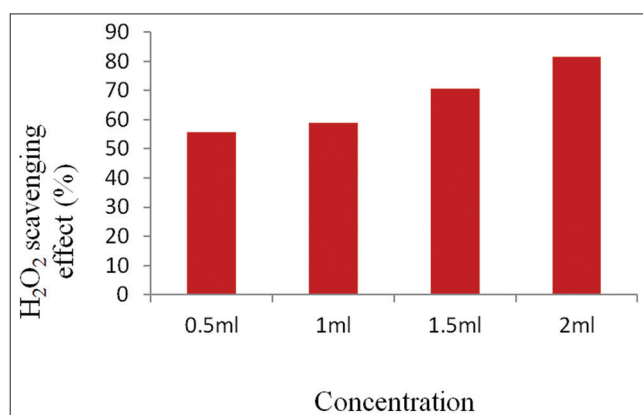


Fig. 2: Antioxidant assay for the extract of *Centella asiatica*

### FTIR spectroscopy

The IR spectroscopic analysis used to determine the chemical functional groups in the sample FTIR spectrum of PVP-coated iron oxide nanoparticle, *C. asiatica* plant extracts, and drug-loaded PVP-coated iron nanoparticles. Fig. 4a represents the fingerprint of  $\text{Fe}_3\text{O}_4$  nanoparticles occurring mainly at 618/cm and the broad absorption 3320/cm represent the stretch vibration of O-H bonds in hydroxyl groups which is absorbed by  $\text{Fe}_3\text{O}_4$  nanoparticles. The small narrow peak at 2359/cm assigned to surface bulk O-H group in magnetite. PVP-coated iron oxide nanoparticle has a carbonyl group characteristic absorption at 1633/cm and 1657/cm. The samples with polymer coating red-shifted from 1660/cm and 1606/cm at a stretching mode, respectively (Fig. 4b). Fig. 4c represents the FTIR spectrum of *C. asiatica* with a strong peak at 1017/cm. OH bond indicates a broad peak at 3331/cm. Stretching frequency of alkyl group peak was shown at 1651/cm and 1450/cm. C-H bond indicates peak at 2929/cm and 2836/cm. Drug loaded iron oxide nanoparticles showed a broad peak at 3313/cm. The strong peak at 1014 and 1646/cm indicated C-O bond. Polymer-coated iron oxide nanoparticles.

### Particle size analysis

The particle size distribution of iron oxide nanoparticle, polymer-coated iron oxide nanoparticle, and drug-loaded polymer-coated iron oxide nanoparticle were shown in Fig. 5a-c. The comparison of uncoated iron oxide nanoparticles with the polymer-coated iron oxide nanoparticles. Iron oxide nanoparticle shows the mean size of 198 nm while the polymer-coated iron oxide nanoparticle showed particle size as 202 nm. Drug loaded iron oxide nanoparticle shows size as 275 nm.

### Drug loading efficiency

In *C. asiatica*, the drug entrapment efficiency was calculated using UV-visible spectroscopy in 1 hr and 24 hrs. Drug loaded uncoated iron oxide nanoparticle have an efficiency of 75% at 24 hrs and drug loaded PVP-coated iron oxide nanoparticles with 78% at 24 hrs. The details can be observed from the Fig. 6a-d.

### X-ray diffraction (XRD) studies

Fig. 7a and b show the XRD curves of Iron oxide nanoparticles both in polymer uncoated and coated forms, respectively. The main peak absorbed at  $2\theta = 19^\circ$  respectively. The XRD spectrum revealed a high degree of crystallinity of the iron oxide nanoparticle. The powder XRD was performed at room temperature with a Cu K $\alpha$  radiation sources ( $\lambda = 0.154056$  nm). XRD pattern of  $\text{Fe}_3\text{O}_4$  confirms the crystallinity of  $\text{Fe}_3\text{O}_4$  nanoparticles. Using the Scherrer's equation, the crystalline grain diameter of the  $\text{Fe}_3\text{O}_4$  particle was determined. The main peak of  $\text{Fe}_3\text{O}_4$  nanoparticle was observed at  $2\theta = 30^\circ, 35.5^\circ, 43^\circ, 53.5^\circ, 57^\circ, 62^\circ$  correspond to 111, 311, 400, 511, and 440, respectively.

### TEM

The TEM image of iron oxide nanoparticle, PVP-coated iron oxide nanoparticle, and drug loaded iron oxide nanoparticle are represented in Fig. 8a-c. 3-30 nm range of mean particle size obtained for iron oxide nanoparticle. The mean particle size obtained for PVP-coated iron oxide nanoparticles was in the range of 40-70 nm. Mean particle size obtained for the drug loaded iron oxide nanoparticles are in the range of 83-110 nm.

### MTT assay for evaluation of apoptosis

The MTT assay was done against fibroblast cell lines (L929) and breast cancer cell lines (MCF-7). The MTT assay results revealed higher cell death in breast cancer cell lines (MCF-7) than fibroblast cell lines when the drug and the nanoparticles were supplied at different concentrations. The results of the cell distribution with confocal microscopy after treatment with the samples are represented in Fig. 9a-d. for the cell lines L929. The details of the cancer cell lines are represented in Fig. 10a-d. Table 1 represents the percentage of cell viability for the given cell lines for different concentrations of the sample. At the concentration of 10  $\mu\text{l}$ , *C. asiatica* loaded iron oxide

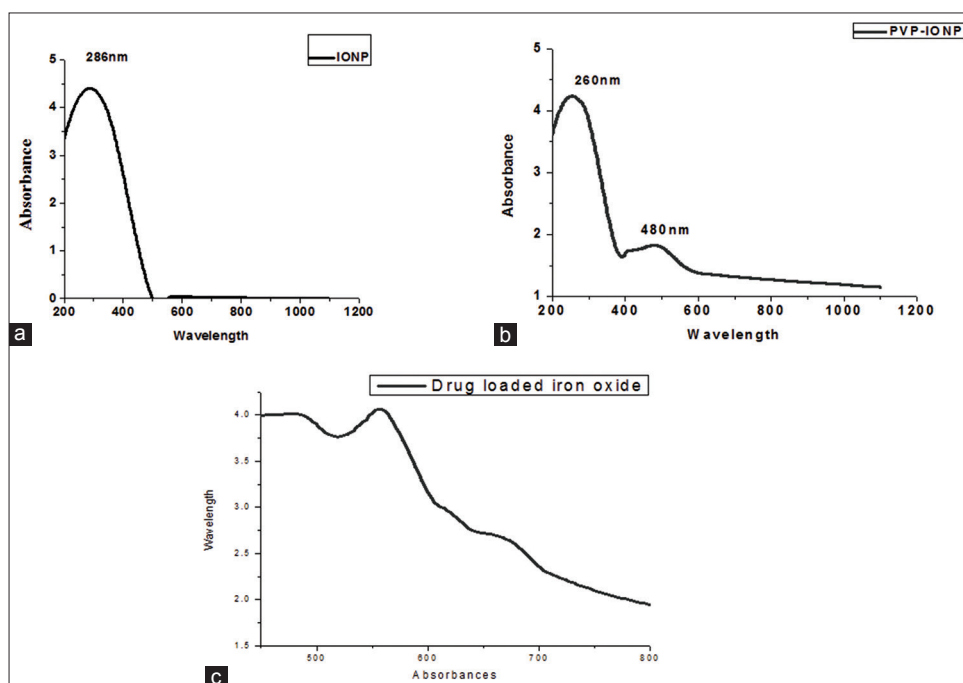


Fig. 3: UV-visible spectroscopic studies of the samples. (a) UV-vis spectra of iron oxide nanoparticles (IONP), (b) UV-vis spectra of polyvinylpyrrolidone-coated IONP, (c) UV-vis spectra of drug loaded IONP

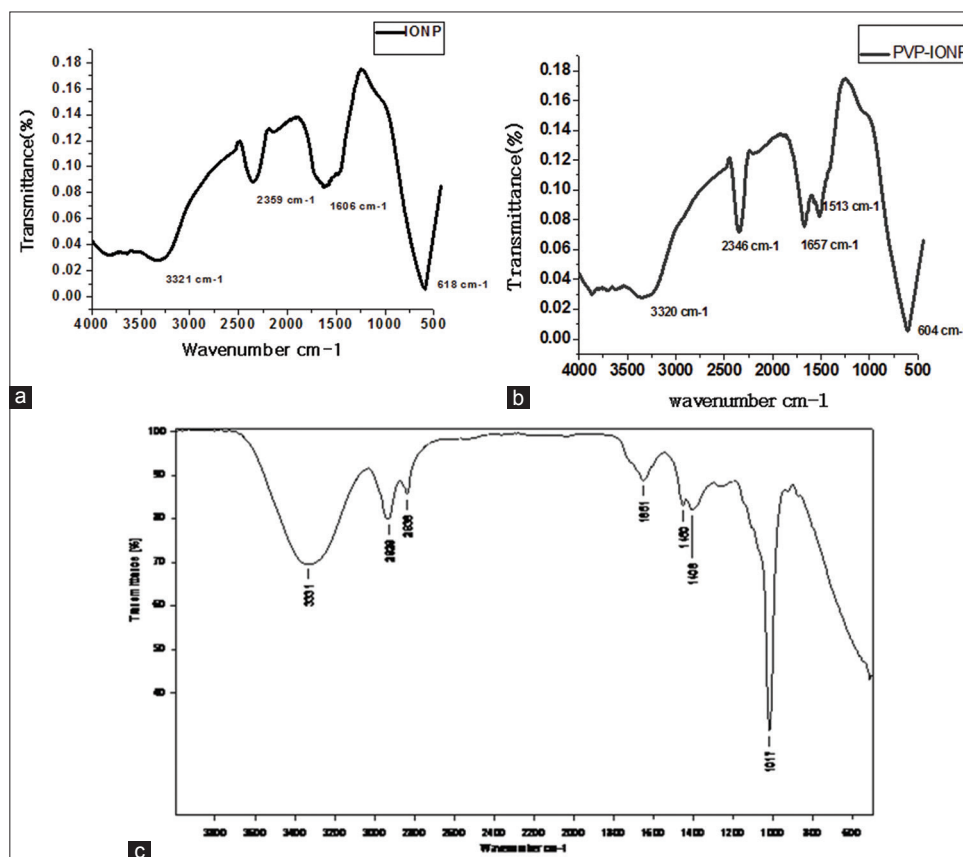


Fig. 4: Fourier transform infra-red spectroscopy (FTIR) spectroscopy of the samples. (a) FTIR spectra of iron oxide nanoparticles, (b) FTIR spectra of polyvinylpyrrolidone (PVP)-coated iron oxide nanoparticles, (c) FTIR of extracts of drug loaded PVP-coated iron oxide nanoparticles

nanoparticle has high cell death as 60% in MCF-7 and 40% in the normal cell line (L929). 10 $\mu$ l of *C. asiatica* had shown a 49.8% in MCF-7

and 29.6% in L929 cell lines. The obtained data are compared with the standard drug 5-fluorouracil.



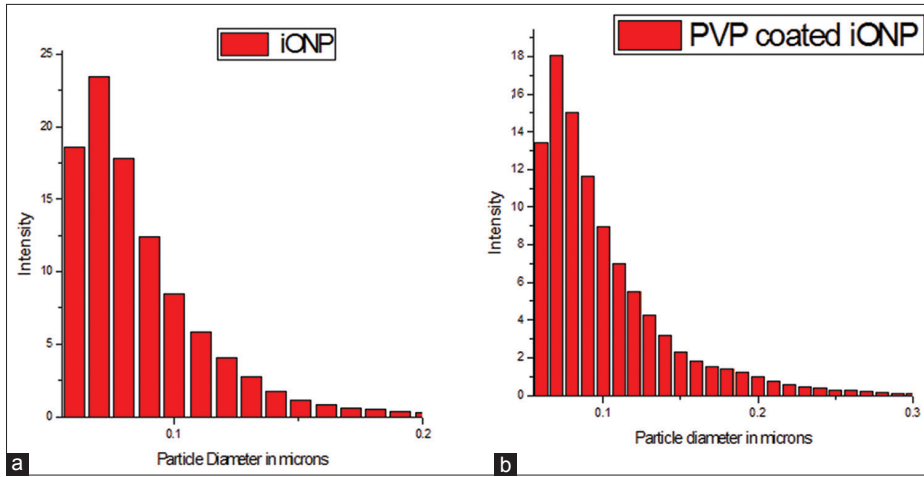


Fig. 5: Determination of the particle size for the synthesized nanoparticles. (a) Particle size analysis of iron oxide nanoparticles (IONP), (b) Particle size analysis of polyvinylpyrrolidone (PVP)-coated IONP, (c) Particle size analysis of extracts of drug loaded PVP-coated IONP

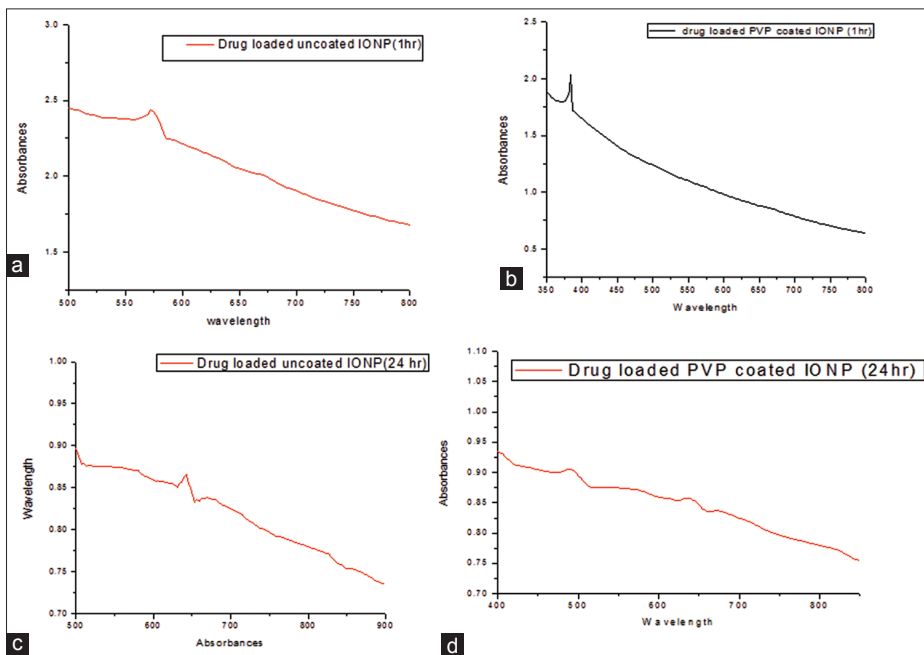


Fig. 6: Analyses of drug entrapment efficiencies of different samples at 1 hr and 24 hrs intervals. (a) Drug entrapment of iron nanoparticles at 1 hr, (b) Drug entrapment of polymer-coated iron nanoparticles at 1 hr, (c) Drug entrapment of iron nanoparticles at 24 hrs, (d) Drug entrapment of polymer-coated iron nanoparticles at 24 hrs

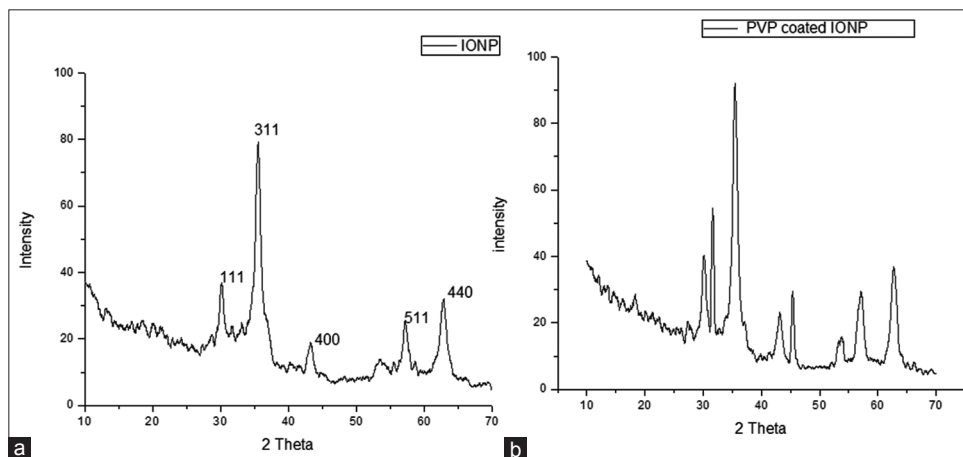
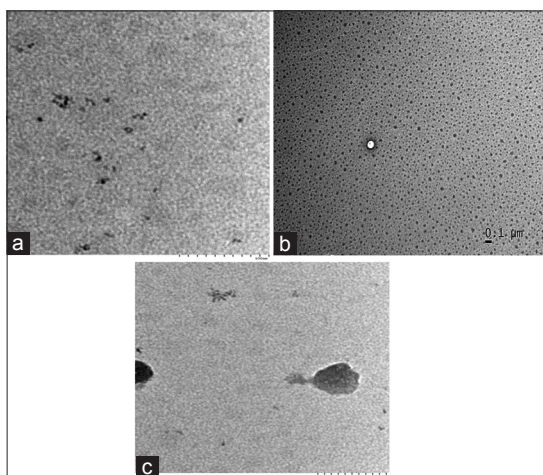
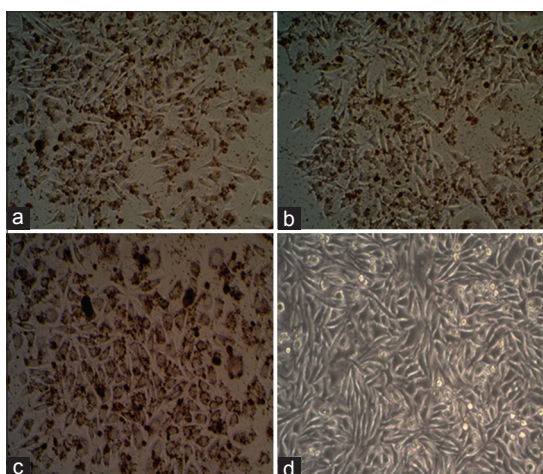


Fig. 7: X-ray diffraction (XRD) analysis of the synthesized nanoparticles. (a) XRD spectra of  $Fe_3O_4$ , (b) XRD spectra of polyvinylpyrrolidone coated  $Fe_3O_4$



**Fig. 8:** Transmission electron microscopic (TEM) images of the synthesized nanoparticles. (a) TEM image of synthesized iron oxide nanoparticles (IONP), (b) TEM image of polymer-coated iron oxide nanoparticles, (c) TEM image of drug loaded IONP



**Fig. 9:** Cytotoxic study on Normal (L929) cell lines - Confocal microscopic images of cell distribution after treatment with drug loaded iron oxide nanoparticles. (a) Concentration-1 µl, (b) Concentration-5 µl, (c) Concentration-10 µl, (d) Control

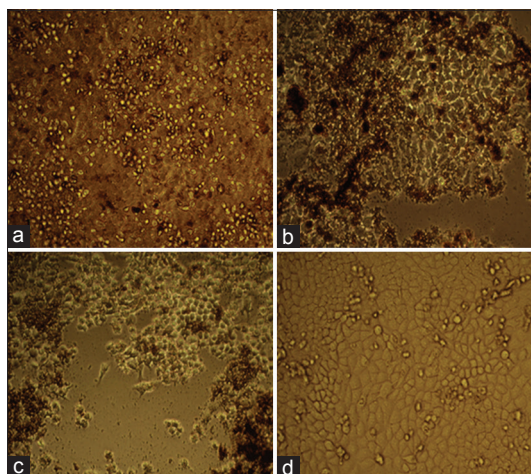


**Fig. 10:** Cytotoxic study of breast cancer cell lines - (michigan cancer foundation - 7 type) - confocal microscopic images of cell distribution after treatment with drug loaded iron oxide nanoparticles. (a) Concentration-1 µl, (b) Concentration-5 µl, (c) Concentration-10 µl, (d) Control

**Table 1:** Percentage viabilities of different cell lines used for cytotoxic studies

Percentage cell viability			
Name of the sample	Concentration	Normal cell-(L929)	Cancer cell-(MCF-7)
IONP	1 µl	98.2	67.32
	5 µl	98	58.90
	10 µl	90.1	51.67
DLIONP	1 µl	70	68
	5 µl	69	50
	10 µl	60	40
<i>C. asiatica</i> (drug)	1 µl	76	64
	5 µl	74	55
	10 µl	70.4	50.2
5-fluorouracil	1 µl	70.1	89.8
	5 µl	69.8	86.3
	10 µl	65	80.9

*C. asiatica*: *Centella asiatica*, IONP: Iron oxide nanoparticles, DLIONP: Drug loaded iron oxide nanoparticles

## DISCUSSIONS

Nanoparticle-based cancer drug research pays attention to the scientific community because of their novel, intrinsic physical properties, and their abilities to target specific cells and mainly for minimizing severe side effects [22]. The most important thing is the functional, and structural properties of the nanosized particles are not seen in discrete molecules or in bulk materials. Several applications of nanoscale compounds were implemented in current clinical therapeutic such as biodegradable nanostructure for drug delivery, iron oxide nanocrystals for magnetic resonance imaging, quantum dots for multiplexed molecular diagnosis and *in vivo* imaging and nanoscale carriers for short interfering RNA (si-RNA) delivery [23]. In this study, we used a methanol extract of *C. asiatica* loaded PVP-coated iron oxide nanoparticle against human breast cancer cell lines MCF-7.

Initially, dose-dependent hydrogen peroxide free radical scavenging activity was carried out for a methanol extract of *C. asiatica* 80% inhibition, respectively. From this, it's clear the hydrogen peroxide activity increases when the concentration of the sample increases. Inhibition of hydrogen peroxide scavenging activity is an important principle for cancer drugs. Hydrogen peroxide initiated the cancer development by means of converting the reactive hydroxyl radicals, which are connected with DNA damage, mutation, and genetic instability [24]. The results were clear that antioxidant principle of the secondary metabolites present in the plant sample may act as chemo-defensive by keeping  $H_2O_2$  levels under physiological level and prevent the cellular or metabolic damage and resembles the character of a chemotherapeutic drug.

The UV spectrum analysis confirmed the drug loading efficiency of the PVP-coated iron oxide nanoparticle with the methanol extract of the *C. asiatica* showed efficiency at 78% compared to uncoated iron oxide nanoparticles efficiency 75% after 24 hrs.

FTIR results confirmed drug loaded polymer PVP-coated iron oxide nanoparticle with the methanolic extracts of *Centella asiatica* shown carbonyl group absorption at 1633/cm and 1657/cm, respectively. Stretching mode exhibited a red-shift from 1660/cm and 1606/cm, respectively. PVP has O and N atom in its five-atom ring, and they can associate with the metal oxide on the nanoparticle crystals. The average particle size estimated for the PVP-coated iron oxide nanoparticle size was obtained in the range of 17-35 nm. While the particle size 202 nm was obtained for methanol extract of *C. asiatica* loaded PVP-coated iron oxide nanoparticle. In this drug loaded PVP-coated iron oxide nanoparticle increases in size when compared to iron oxide coated particles; this will be due to the coating of polymer along with the drug gradually increasing the size.

The cell line assay is the most important method to analyze various expose of cell necrosis to provide information about the cell death, survival rate, and metabolic activity [25]. *In vitro* studies of drug loaded PVP-coated iron oxide nanoparticles were analyzed in normal cell lines (L929) and breast cancer cell lines (MCF-7). At 10 µl concentrations of methanol extract of methanol extract of *C. asiatica* loaded PVP-coated iron oxide nanoparticle shown 60% cell necrosis in breast cancer cell lines (MCF-7) compare to *C. asiatica* methanol extract loaded iron oxide nanoparticle as 48.33%, respectively. The anticancer activity of standard compound are low as 19.1% compared to methanol extract of *C. asiatica* loaded PVP-coated iron oxide nanoparticle and methanol extract of *C. asiatica*. There are many reports stating that the efficiency of the polymer-coated iron oxide nanoparticle along with the drug molecule will act as the cell-specific delivery and kill the uptake cancer cells [26,27].

## CONCLUSION

Our study makes another proof the efficiency of the methanol extract of *C. asiatica* loaded PVP-coated iron oxide nanoparticle act as the effective against breast cancer. The overall results make clear that *C. asiatica* loaded PVA-coated iron oxide nanoparticles will be the effective alternative drug to treat cancer, and the results make another conclusion that drug coated with the nanoparticle may lead to greater impact in the cancer clinical area as target-based drug delivery.

## ACKNOWLEDGMENTS

The Authors thank Noorul Islam Centre for Higher Education, Thuckalay, Tamil Nadu, India for providing all possible research facilities.

## REFERENCES

- Mitra AK, Faruque FS. Breast cancer incidence and exposure to environmental chemicals in 82 counties in Mississippi. *South Med J* 2004;97(3):259-63.
- Desai SB, Moonim MT, Gill AK, Punia RS, Naresh KN, Chinoy RF. Hormone receptor status of breast cancer in India: A study of 798 tumours. *Breast* 2000;9(5):267-70.
- Brody JG, Moysich KB, Humblet O, Attfield KR, Beehler GP, Rudel RA. Environmental pollutants and breast cancer: Epidemiologic studies. *Cancer* 2007;109 12 Suppl:2667-711.
- Smith RA, Caleffi M, Albert US, Chen TH, Duffy SW, Franceschi D, et al. Breast cancer in limited-resource countries: Early detection and access to care. *Breast J* 2006;12 Suppl 1:S16-26.
- Wang X, Wei Y, Yuan S, Liu G, Lu Y, Zhang J, et al. Potential anticancer activity of tanshinone IIA against human breast cancer. *Int J Cancer* 2005;116(5):799-807.
- Yezhelyev MV, Gao X, Xing Y, Al-Hajj A, Nie S, O'Regan RM. Emerging use of nanoparticles in diagnosis and treatment of breast cancer. *Lancet Oncol* 2006;7(8):657-67.
- Wagner V, Dullaart A, Bock AK, Zweck A. The emerging nanomedicine landscape. *Nat Biotechnol* 2006;24(10):1211-7.
- Sriram MI, Kanth SB, Kalishwaralal K, Gurunathan S. Antitumor activity of silver nanoparticles in Dalton's lymphoma ascites tumor model. *Int J Nanomedicine* 2010;5:753-62.
- Brigger I, Dubernet C, Couvreur P. Nanoparticles in cancer therapy and diagnosis. *Adv Drug Deliv Rev* 2002;54(5):631-51.
- Brown SD, Nativo P, Smith JA, Stirling D, Edwards PR, Venugopal B, et al. Gold nanoparticles for the improved anticancer drug delivery of the active component of oxaliplatin. *J Am Chem Soc* 2010;132(13):4678-84.
- Liu Y, Miyoshi H, Nakamura M. Nanomedicine for drug delivery and imaging: A promising avenue for cancer therapy and diagnosis using targeted functional nanoparticles. *Int J Cancer* 2007;120(12):2527-37.
- Berry CC, Curtis AS. Functionalization of magnetic nanoparticles for applications in biomedicine. *J Phys Appl Phys* 2003;36(13):198. Available from: <http://www.iopscience.iop.org/article/10.1088>.
- Nel A, Xia T, Mädler L, Li N. Toxic potential of materials at the nanolevel. *Science* 2006;311(5761):622-7.
- Yigit MV, Moore A, Medarova Z. Magnetic nanoparticles for cancer diagnosis and therapy. *Pharm Res* 2012;29(5):1180-8.
- Jain TK, Morales MA, Sahoo SK, Leslie-Pelecky DL, Labhasetwar V. Iron oxide nanoparticles for sustained delivery of anticancer agents. *Mol Pharm* 2005;2(3):194-205.
- Gohil KJ, Patel JA, Gajjar AK. Pharmacological review on *Centella asiatica*: A potential herbal cure-all. *Indian J Pharm Sci* 2010;72(5):546-56.
- Babu TD, Kuttan G, Padikkala J. Cytotoxic and anti-tumour properties of certain taxa of Umbelliferae with special reference to *Centella asiatica* (L.) Urban. *J Ethnopharmacol* 1995;48(1):53-7.
- Singh N, Manshian B, Jenkins GJ, Griffiths SM, Williams PM, Maffei TG, et al. nanogenotoxicology: The DNA damaging potential of engineered nanomaterials. *Biomaterials* 2009;30(23-24):3891-914.
- Yu H, Xu X, Chen X, Lu T, Zhang P, Jing X. Preparation and antibacterial effects of PVA-PVP hydrogels containing silver nanoparticles. *J Appl Polym Sci* 2007;103(1):125-33. Available from: <http://www.onlinelibrary.wiley.com/doi/10.1002/app.24835/>.
- Nishikawa M, Huang L. Nonviral vectors in the new millennium: Delivery barriers in gene transfer. *Hum Gene Ther* 2001;12(8):861-70.
- Harborne AJ. *Phytochemical Methods A Guide to Modern Techniques of Plant Analysis*. Springer Science and Business Media; 1998. Available from: [https://www.books.google.co.in/books/about/Phytochemical\\_Methods\\_A\\_Guide\\_to\\_Modern.html](https://www.books.google.co.in/books/about/Phytochemical_Methods_A_Guide_to_Modern.html).
- Rahmatullah M, Das AK, Mollik MA, Jahan R, Khan M, Rahman T, et al. An ethno medicinal survey of Dhamrai sub-district in Dhaka district, Bangladesh. *Am Eurasian J Sustain Agric* 2009;3(4):881-8. Available from: <http://www.researchgate.net/publication/228673477>.
- Qian X, Peng XH, Ansari DO, Yin-Goen Q, Chen GZ, Shin DM, et al. *In vivo* tumor targeting and spectroscopic detection with surface-enhanced Raman nanoparticle tags. *Nat Biotechnol* 2008;26(1):83-90.
- Tang EL, Rajarajeswaran J, Fung SY, Kanthimathi MS. Antioxidant activity of Coriandrum sativum and protection against DNA damage and cancer cell migration. *BMC Complement Altern Med* 2013;13(1):347.
- Shukla A, Rasik AM, Jain GK, Shankar R, Kulshrestha DK, Dhawan BN. *In vitro* and *in vivo* wound healing activity of asiaticoside isolated from *Centella asiatica*. *J Ethnopharmacol* 1999;65(1):1-11.
- Sunitha A, Praseetha PK. Diagnostics and treatment of metastatic cancers with magnetic nanoparticles. *J Nanomed Biother Discov* 2013;3(2):115-25. Available from: <http://www.omicsonline.org/2155-983X.1000115.php>.
- Jana D, Radim H, Vojtech A, Rene K, Oldrich S, Jaromir H. Preparation and properties of various magnetic nanoparticles. *Sensors* 2009;6:2352-62. Available from <http://www.mdpi.com/1424-8220/9/4/2352>.